FEBS 26028

FEBS Letters 518 (2002) 39–42

The importance of the conserved Arg191–Asp227 salt bridge of triosephosphate isomerase for folding, stability, and catalysis

Inari Kursula[a], Sanna Partanen[a], Anne-Marie Lambeir[b], Rik K. Wierenga[a,*]

[a] *Department of Biochemistry and Biocenter Oulu, University of Oulu, P.O. Box 3000, FIN-90014 Oulu, Finland*
[b] *Laboratory of Medical Biochemistry, University of Antwerp, Universiteitsplein 1, B-2610 Antwerp, Belgium*

Received 4 February 2002; revised 20 March 2002; accepted 22 March 2002

First published online 9 April 2002

Edited by Hans Eklund

Abstract **Triosephosphate isomerase (TIM) has a conserved salt bridge 20 Å away from both the active site and the dimer interface. In this study, four salt bridge mutants of *Trypanosoma brucei brucei* TIM were characterized. The folding and stability of the mutants are impaired compared to the wild-type enzyme. This salt bridge is part of a hydrogen bonding network which tethers the C-terminal β7α7β8α8 unit to the bulk of the protein. In the variants D227N, D227A, and R191S, this network is preserved, as can be deduced from the structure of the R191S variant. In the R191A variant, the side chain at position 191 cannot contribute to this network. Also the catalytic power of this variant is most affected.** © **2002 Federation of European Biochemical Societies. Published by Elsevier Science B.V. All rights reserved.**

Key words: Triosephosphate isomerase; Salt bridge; Folding; Stability; Kinetics

1. Introduction

Salt bridges are important for the folding, stability, and function of proteins. Experimental studies [1] and biocomputational calculations [2,3] suggest that salt bridges can have both stabilizing and destabilizing contributions to the overall stability of a protein. Comparative sequence and structural studies on triosephosphate isomerase (TIM) have shown that it has a fully conserved salt bridge, the function of which is not understood [4,5]. Recently, random mutagenesis experiments on TIM have also highlighted the importance of this salt bridge [6].

TIM is a well conserved dimeric protein, consisting of two identical subunits of 250 residues. The active site is located at the C-terminal end of the β-strands of a $(\beta\alpha)_8$ barrel fold. The core of the barrel is composed of eight parallel β-strands, labeled from the N-terminus to the C-terminus as β1–β8. The corresponding α-helices around the exterior are labeled as α1–α8. The loops connecting the β-strands to the subsequent helices are called loops 1–8. A prominent feature of the active site is the conformational flexibility of loops 6 and 7. Loop 6 closes the substrate in, adopting a conformation differing by 7 Å from the open state [7–9]. In loop 7, two peptide planes adopt different orientations in the open and closed conformation [9]. The key catalytic residue, glutamate 167, lies at the very beginning of loop 6, and its side chain also goes through a conformational change as the substrate is bound [9,10].

TIM contains a number of fully conserved residues, most of which are either catalytic residues or directly interacting with the active site. An exception is the conserved salt bridge between Arg191 and Asp227, approximately 20 Å away from both the nearest active site and the dimer interface. This salt bridge connects the C-terminal ends of helices 6 and 7 to each other (Fig. 1). The salt bridge-forming residues are fully conserved in about 60 TIM sequences. Arg191 is in helix 6, and Asp227 is the first D of a conserved DX(D/N)G motif in the C-terminal end of helix 7, just before strand 8. In the vicinity of this salt bridge, there are several other residues that form a crucial hydrogen bonding network (Figs. 2 and 3), which links the C-terminal β7α7β8α8 unit to the rest of the protein.

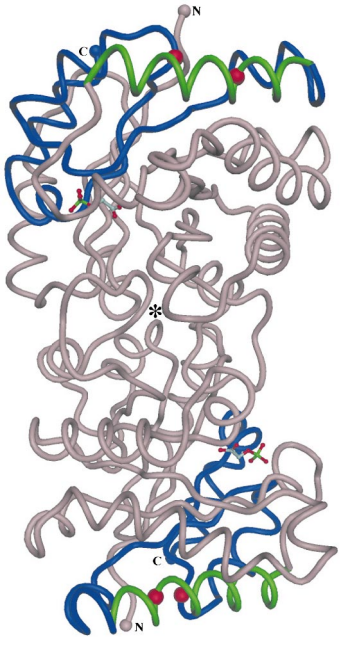

Fig. 1. An overview of the TIM dimer viewed approximately down the dimer two-fold axis (marked with an asterisk). The salt bridge is located at the far end from the dimer interface. The salt bridge residues (Arg191 and Asp227) are shown as red spheres. α-Helix 6 is colored green, the N-terminal part of the protein is colored pink, and the C-terminus blue. The bound inhibitor, PGA, depicted as a ball-and-stick model, identifies the active site of both subunits.

*Corresponding author. Fax: (358)-8-5531141.
E-mail address: rik.wierenga@oulu.fi (R.K. Wierenga).

Abbreviations: DHAP, dihydroxyacetone phosphate; GAP, glyceraldehyde-3-phosphate; GuHCl, guanidinium hydrochloride; PGA, 2-phosphoglycolate; TIM, triosephosphate isomerase

PII: S0014-5793(02)02639-X

Gly230 in the DX(D/N)G motif is also 100% conserved, which correlates with its phi/psi values of 130/−171, only allowed for glycines. The residue at the X-position is always small and hydrophobic, such as alanine, valine, or isoleucine, and the side chain is pointing inwards to a hydrophobic cluster that includes Leu232 near the active site. The salt bridge is rather buried; residue 229 is almost fully buried, whereas 227 is somewhat more exposed (Fig. 2).

In this work, we have studied the role of the conserved salt bridge by mutating the key residues (Arg191 and Asp227) in the *Trypanosoma brucei brucei* TIM and studying the kinetic and structural properties of these variants.

2. Materials and methods

2.1. Mutagenesis and protein purification

The point mutations R191A, R191S, D227A, and D227N were introduced to the wild-type *T. brucei brucei* TIM sequence using the QuikChange™ site-directed mutagenesis kit (Stratagene, La Jolla, CA, USA). Protein expression and purification were performed as described before [11], omitting the ammonium sulfate precipitation step. The mutants D227A and R191A had to be solubilized by adding 1% Triton X-100 to the lysis buffer. The mutants were soluble when expressed at low temperature (15–20°C), but the expression levels were low compared to the wild-type enzyme.

2.2. Enzyme kinetics

Kinetic parameters for D-glyceraldehyde-3-phosphate (D-GAP) and dihydroxyacetone phosphate (DHAP) were determined as described before [12] except that the measurements were done in a Spectramax 340 microtiter plate reader (Molecular Devices, Sunnyvale, CA, USA) in a volume of 80 μl, using narrow 96-well microtiter plates (Costar, Bucks, UK). The formation of methylglyoxal was measured according to Gawehn and Bergmeyer [13]. D,L-GAP, DHAP, and 2-phosphoglycolate (PGA) were from Sigma, glycerolphosphate dehydrogenase and GAP dehydrogenase were from Roche.

2.3. Denaturation and refolding studies

Melting curves were measured at 222 nm with a Jasco J-715 circular dichroism spectropolarimeter (Jasco Corporation, Tokyo, Japan). The sample contained 0.2 mg/ml protein in 20 mM 3-(*N*-morpholino)propanesulfonic acid buffer (pH 7.0) containing 0.02 mM dithiothreitol, 0.02 mM ethylenediaminetetraacetic acid, and 0.02 mM sodium azide. The heating rate was 1°C/min. Thermoinactivation kinetics were determined by enzyme activity measurements after incubation of 1 μg/ml of protein at 42°C in 100 mM triethanolamine buffer (pH 7.6) containing 1 mM dithiothreitol and 0.1 mg/ml bovine serum albumin. The kinetics of unfolding in 3.2 M guanidinium hydrochloride (GuHCl) were monitored by fluorescence at 25°C using 20 μg/ml of protein in 100 mM triethanolamine buffer (pH 7.8). For measuring the refolding kinetics, the unfolded protein samples were diluted to final concentrations of 0.32 M GuHCl and 2 μg/ml protein in 100 mM triethanolamine buffer (pH 7.6) containing 1 mM dithiothreitol and 0.1 mg/ml bovine serum albumin. The recovery of activity was monitored by enzyme activity measurements.

2.4. Crystallographic studies

Crystallization of the R191S mutant was carried out at room temperature, using the hanging drop vapor diffusion method. The crystals were grown from a mother liquor containing 2 M ammonium sulfate, 0.1 M citric acid (pH 5.5), and 0.2 M NaCl. The protein solution contained 3 mg/ml protein and 10 mM PGA. 20% glycerol was used as the cryo protectant, and the crystal was flash-frozen in the cryostream. A data set was collected at 1.65 Å resolution from a single crystal at 100 K at beam line X13 at the EMBL outstation, DESY, Hamburg, Germany, on a MAR CCD detector. The data were processed with Denzo and Scalepack [14]. Further data reduction was done with programs of the CCP4 package [15]. The data collection statistics are shown in Table 1. The structure was solved by molecular replacement with the program AMoRe [16] using the wild-type *T. brucei brucei* TIM structure (5TIM) as the search model. The structure was refined with REFMAC5 [17] using translation, libration, and screw-rotation parameterization [18], and water molecules were added using ARP/wARP [19]. The refinement resulted in a model with good geometry and *R*-free and *R*-values of 17.5% and 14.3%, respec-

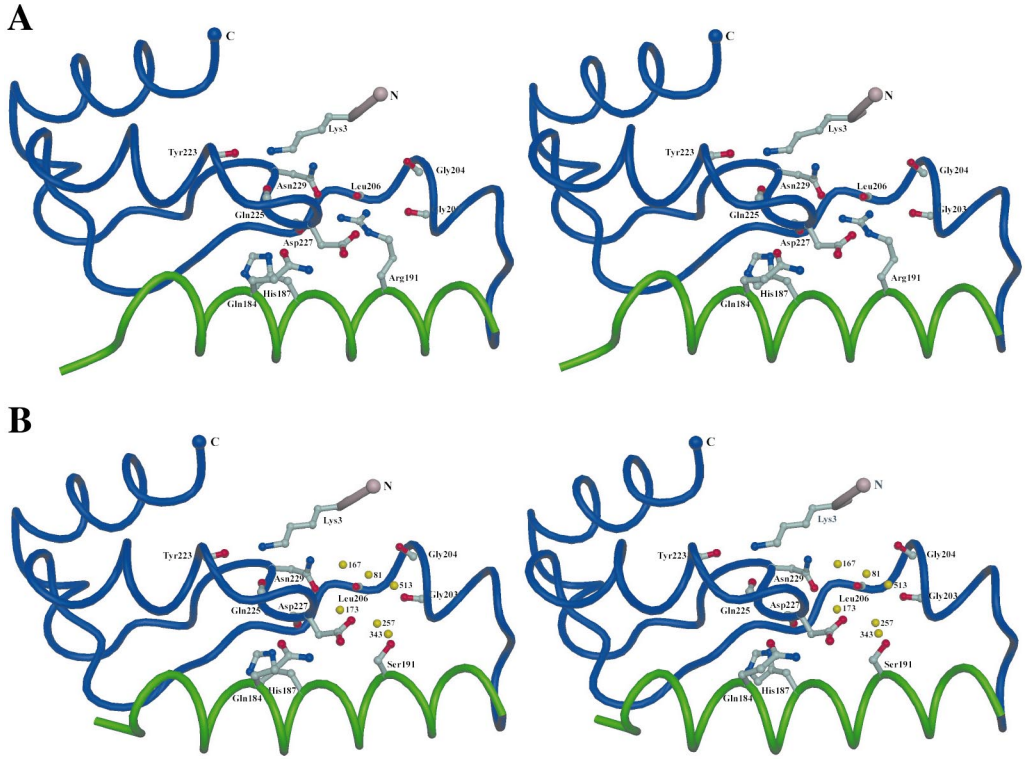

Fig. 2. Details of the geometry of the salt bridge and the adjacent hydrogen bonding network in wild-type (5TIM) (A) and R191S mutant (1KV5) (B). The N-terminus is colored pink, the C-terminal part blue, and α-helix 6 green. The side chains of the key residues are labeled. The water molecules, presented as yellow spheres, in (B) are well defined and observed in both subunits. The figure was generated with DINO [31].

tively (Table 1). The program O [20] was used for model building. The quality of the model was analyzed with PROCHECK [21].

3. Results and discussion

Kinetic, stability, and folding properties were determined for four salt bridge mutants that partially or completely abolish the interaction between the side chains of Arg191 and Asp227 in *T. brucei brucei* TIM. In addition, the crystal structure of the R191S variant complexed with PGA was determined at 1.65 Å resolution.

The side chain of serine 191 is well defined in the crystal structure, and hydrogen bonds to water molecules have partly compensated for the loss of the salt bridge. Other hydrogen bonding contacts in the area have also been preserved by this water-mediated network (Figs. 2 and 3). Apart from the mutation and the new water molecules, there are no structural changes in the area. In the R191A variant, the hydrogen bonding network has to deviate more from the wild-type enzyme, due to the lack of a suitable hydrogen bond donor or acceptor in the side chain at position 191.

The variant R191A displays the largest differences in the catalytic properties (Table 2). For example, its k_{cat}/K_m value is 10-fold lower than that for wild-type TIM. The mutants do not show an increase in methylglyoxal synthase activity, indicating that the closed conformation of loops 6 and 7 is not affected by the mutations [22]. In good agreement with the high structural similarity, the inhibition constant of PGA for the R191S mutant was 60 μM (competitive inhibition), as in the wild-type enzyme [12]. According to the T_m values, the overall stability of the mutants has somewhat decreased compared to the wild-type enzyme (Table 2). The largest difference is seen for the R191A mutant, for which the T_m value has decreased by 5°C. All four salt bridge mutants show higher rates of thermoinactivation and unfolding under denaturing conditions, as well as less complete recovery of activity after refolding, when compared to the wild-type enzyme (Table 2).

Table 1
Data collection and refinement statistics of the R191S mutant of *T. brucei brucei* TIM (1KV5)

Space group	$P2_12_12_1$
Cell dimensions (Å)	44.94×100.64×109.35
Cell dimensions (°)	90, 90, 90
Subunits per asymmetric unit	2
V_m (Å^3/Da)	2.3
Data collection statistics	
Observed reflections	245 458
Unique reflections	60 451
Resolution range (Å)	15–1.65
Completeness (%)	99.9 (99.3)
I/σ	37.7 (5.4)
R-merge (%)	3.1 (25.3)
Refinement statistics	
Protein atoms	3848
Ligand atoms	18
Solvent atoms	818
R-factor (%)	14.3
Free *R*-factor (%)	17.5
Rms deviation from ideal geometry:	
Bond lengths (Å)	0.013
Bond angles (°)	1.77
Temperature factors:	
Average *B* (main chain) (Å^2)	16.0
Average *B* (side chain) (Å^2)	18.6
Average *B* (solvent) (Å^2)	34.0
Rms Δ*B* of bonded atoms (main chain) (Å^2)	0.596
Rms Δ*B* of bonded atoms (side chain) (Å^2)	1.756

Values in parentheses correspond to the highest resolution shell (1.68–1.65 Å).

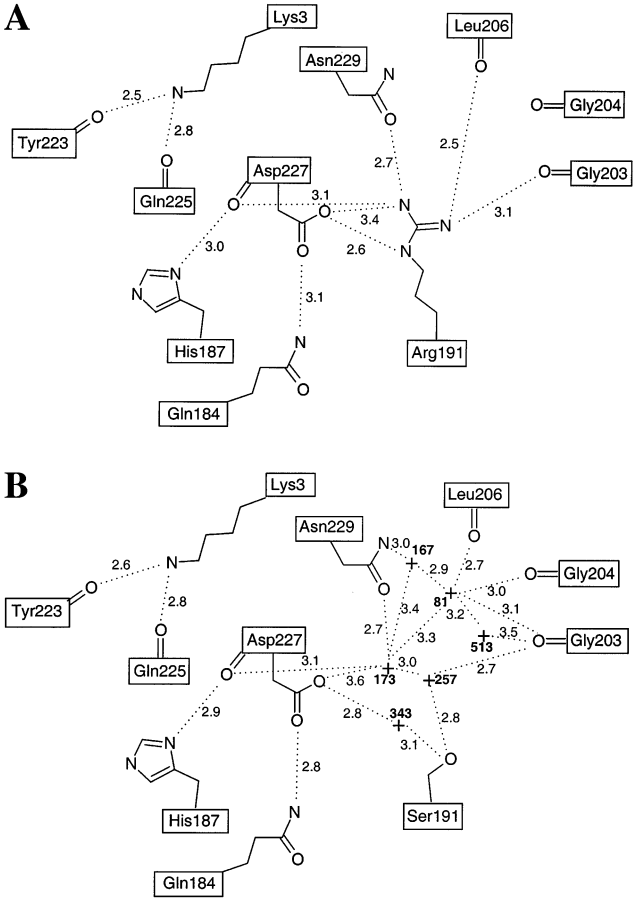

Fig. 3. Distance information concerning the salt bridge area in wild-type (5TIM) (A) and the R191S mutant (1KV5) (B). Water molecules in (B) are identified by a +.

The removal of the salt bridge causes subtle changes in the stability and catalytic properties of the enzyme, especially in the case of the R191A mutant. In particular, though, it seems to deteriorate the (re)folding kinetics. Assuming that the structural differences are minimal, as can be seen for the R191S mutant, the effect on catalysis is intriguing as the hydrogen bonding network is 20 Å away from the active site. Its importance for catalysis would be consistent with the full evolutionary conservation of the salt bridge, suggesting that some long distance effects, such as electrostatics [23] or dynamics [24] are important for obtaining optimal active site properties. The salt bridge and the related hydrogen bonding network anchor the C-terminal ends of helices 6 and 7 to each other. However, from the present data, it is not clear whether this could influence the dynamical properties of the flexible loops 6 and 7 involved in substrate binding. Although the R191A mutant has reduced catalytic activity compared to the wild-type *T. brucei brucei* TIM, it has to be stated that the kinetic constants fall within the range reported for several TIMs from different organisms. It therefore seems unlikely that maintaining the activity is the sole evolutionary pressure for the conservation of this specific interaction.

The salt bridge discussed in this paper is close to the surface of the protein, but it is nevertheless almost completely buried.

Table 2
Kinetic, stability, and folding data of wild-type *T. brucei brucei* TIM and four salt bridge mutants

Parameter	Unit	Wild-type	D227N	D227A	R191S	R191A
K_m (GAP)	mM	0.25	0.28	0.24	0.34	1.1
k_{cat} (GAP)	s^{-1}	6000	1600	2600	4000	2500
k_{cat}/K_m (GAP)	s^{-1} mM^{-1}	24000	5700	11000	12000	2300
K_m (DHAP)	mM	1.0	0.7	0.9	1.6	0.67
k_{cat} (DHAP)	s^{-1}	1000	200	180	240	63
k_{cat}/K_m (DHAP)	s^{-1} mM^{-1}	1000	285	200	150	94
T_m	°C	52.2	49.3	48.7	51.6	47.3
$t_{1/2}$ (42°C)	min	180	128	122	87	124
$t_{1/2}$ (GuHCl)	min	30	20	15	8	19
Recovery of activity (after 0.5 h)	%	4.2	0.9	1.9	2.2	2.2
Recovery of activity (after 4.5 h)	%	10.9	1.6	2.5	2.6	2.8
Recovery of activity (after 24 h)	%	15.9	2.1	2.7	2.6	2.8
Recovery of activity (after 72 h)	%	16.0	2.1	2.8	2.4	2.6

The experimental details are discussed in Section 2.

The amount of charge in the vicinity of the salt bridge varies from organism to organism. On one side of the salt bridge, there is always one positively charged group – arginine, or in some cases lysine. On the other end, there can be either one or two negatively charged groups – the DX(D/N)G motif. Thus, it does not seem likely that changing the charge in this area would be the reason for the loss of enzyme activity. Indeed, mutating both partners of the salt bridge separately and together results in a non-functional enzyme [6].

An increasing number of experimental studies [25,26] and theoretical analyses [27,28] address the folding properties of TIM. Computational approaches have pointed out the importance of folding initiation sites [27], and Gly230 in the DX(D/N)G motif has been postulated to be such a nucleation site [28]. This motif is located at the extremity of the dimer (Fig. 1), and it tethers the C-terminal β7α7β8α8 unit to the rest of the protein via an extensive hydrogen bonding network (Fig. 2). Also the N-terminus participates in this hydrogen bonding scheme (Fig. 2). Apparently, the formation of the Arg191–Asp227 salt bridge in this network is important for efficient folding. This would also explain the low expression yields of the mutants in this study, as well as the loss of functional enzyme in an earlier mutagenesis study [6]. Furthermore, the recovery of activity after refolding (Table 2) is much less effective for the mutants than for the wild-type enzyme. It is interesting to point out that refolding experiments with two monomeric TIM-barrel proteins, phosphoribosylanthranilate isomerase [29] and the α-subunit of tryptophan synthase [30], have shown that, in these proteins, two folding units exist; the βα units 1–6 fold first and subsequently assemble with the βα units 7 and 8 at the end of the folding pathway. Our results on the TIM salt bridge variants indicate that the evolutionary pressure for the conservation of the salt bridge is due to the requirement for efficient folding of TIM.

Acknowledgements: We thank the staff of the EMBL Hamburg outstation for excellent support during data collection and Dr. Päivi Pirilä for help with the CD measurements. Dr. Petri Kursula is acknowledged for careful reading of the manuscript. The structure factors and coordinates of the R191S mutant structure have been submitted to the protein data bank (PDB entry code 1KV5).

References

[1] Strop, P. and Mayo, S.L. (2000) Biochemistry 39, 1251–1255.
[2] Hendsch, Z.S. and Tidor, B. (1994) Protein Sci. 3, 211–226.
[3] Kumar, S. and Nussinov, R. (2001) Proteins Struct. Funct. Genet. 43, 433–454.
[4] Wierenga, R.K., Noble, M.E.M. and Davenport, R.C. (1992) J. Mol. Biol. 224, 1115–1126.
[5] Maes, D., Zeelen, J.P., Thanki, N., Beaucamp, N., Alvarez, M., Thi, M.H.D., Backmann, J., Martial, J.A., Wyns, L., Jaenicke, R. and Wierenga, R.K. (1999) Proteins Struct. Funct. Genet. 37, 441–453.
[6] Silverman, J.A., Balakrishnan, R. and Harbury, P.B. (2001) Proc. Natl. Acad. Sci. USA 98, 3092–3097.
[7] Williams, J.C. and McDermott, A.E. (1995) Biochemistry 34, 8309–8319.
[8] Sampson, N.S. and Knowles, J.R. (1992) Biochemistry 31, 8482–8487.
[9] Noble, M.E., Zeelen, J.P. and Wierenga, R.K. (1993) Proteins Struct. Funct. Genet. 16, 311–326.
[10] Lolis, E. and Petsko, G.A. (1990) Biochemistry 29, 6619–6625.
[11] Schliebs, W., Thanki, N., Jaenicke, R. and Wierenga, R.K. (1997) Biochemistry 36, 9655–9662.
[12] Lambeir, A.M., Opperdoes, F.R. and Wierenga, R.K. (1987) Eur. J. Biochem. 168, 69–74.
[13] Gawehn, K., Bergmeyer, H.U. (1974) in: Methoden der entzymatischen Analyse (Bergmeyer, H.U., Ed.), pp. 1542–1544, Verlag Chemie, Weinheim.
[14] Otwinovski, Z. and Minor, W. (1997) Methods Enzymol. 276, 307–326.
[15] Collaborative Computational Project Number 4 (1994) Acta Crystallogr. D50, 760–763.
[16] Navaza, J. (1994) Acta Crystallogr. A50, 157–163.
[17] Murshudov, G.N., Vagin, A.A. and Dodson, E.J. (1997) Acta Crystallogr. D55, 247–255.
[18] Schomaker, V. and Trueblood, K.N. (1968) Acta Crystallogr. B24, 63–76.
[19] Perrakis, A., Morris, R. and Lamzin, V.S. (1999) Nat. Struct. Biol. 6, 458–463.
[20] Jones, T.A., Zou, J.-Y., Cowan, S.W. and Kjeldgaard, M. (1991) Acta Crystallogr. A47, 110–119.
[21] MacArthur, M.W., Moss, D.S. and Thornton, J.M. (1993) J. Appl. Crystallogr. 26, 283–291.
[22] Pompliano, D.L., Peyman, A. and Knowles, J.R. (1990) Biochemistry 29, 3186–3194.
[23] Fersht, A.C. (1999) in: Structure and Mechanism in Protein Science, 2nd edn., W.H. Freeman, New York.
[24] Wand, A.J. (2001) Nat. Struct. Biol. 8, 926–931.
[25] Morgan, C.J., Wilkins, D.K., Smith, L.J., Kawata, Y. and Dobson, C.M. (2000) J. Mol. Biol. 300, 11–16.
[26] Benítez-Cardoza, C.G., Rojo-Domínguez, A. and Hernández-Arana, A. (2001) Biochemistry 40, 9049–9058.
[27] Mirny, L.A. and Shakhnovich, E.I. (1999) J. Mol. Biol. 291, 177–196.
[28] Kannan, S., Selvaraj, S., Gromiha, M.M. and Vishveshwara, S. (2001) Proteins Struct. Funct. Genet. 43, 103–112.
[29] Eder, J. and Kirscher, K. (1992) Biochemistry 31, 3617–3625.
[30] Zitzewitz, J.A. and Matthews, C.R. (1999) Biochemistry 38, 10205–10214.
[31] Philippsen, A. (2001) http://www.bioz.unibas.ch/~xray/dino.